Molecular Therapy
Methods & Clinical Development
Original Article

Cardiotoxicity assessment using 3D vascularized cardiac tissue consisting of human iPSC-derived cardiomyocytes and fibroblasts

Kiyoshi Tadano,[1] Shigeru Miyagawa,[2] Maki Takeda,[2] Yoshinari Tsukamoto,[3] Katsuyuki Kazusa,[1] Kazuhiko Takamatsu,[1] Mitsuru Akashi,[3] and Yoshiki Sawa[2]

[1]Drug Safety Research Labs, Astellas Pharma Inc., Tsukuba, Ibaraki 305-8585, Japan; [2]Department of Cardiovascular Surgery, Osaka University Graduate School of Medicine, Suita, Osaka 565-0871, Japan; [3]Building Block Science Joint Research Chair, Graduate School of Frontier Biosciences, Osaka University, Suita, Osaka 565-0871, Japan

Human induced pluripotent stem cell-derived cardiomyocytes (hiPSC-CMs) are used for cardiac safety assessment but have limitations for the evaluation of drug-induced contractility. Three-dimensional (3D) cardiac tissues are similar to native tissue and valuable for the assessment of contractility. However, a longer time and specialized equipment are required to generate 3D tissues. We previously developed a simple method to generate 3D tissue in a short period by coating the cell surfaces with extracellular matrix proteins. We hypothesized that this 3D cardiac tissue could be used for simultaneous evaluation of drug-induced repolarization and contractility. In the present work, we examined the effects of several compounds with different mechanisms of action by cell motion imaging. Consequently, human ether-a-go-go-related gene (HERG) channel blockers with high arrhythmogenic risk caused prolongation of contraction-relaxation duration and arrhythmia-like waveforms. Positive inotropic drugs, which increase intracellular Ca^{2+} levels or myocardial Ca^{2+} sensitivity, caused an increase in maximum contraction speed (MCS) or average deformation distance (ADD) (ouabain, 138% for MCS at 300 nM; pimobendane, 132% for ADD at 3 μM). For negative inotropic drugs, verapamil reduced both MCS and ADD (61% at 100 nM). Thus, this 3D cardiac tissue detected the expected effects of various cardiovascular drugs, suggesting its usefulness for cardiotoxicity evaluation.

INTRODUCTION

The cardiovascular system plays an essential role in the maintenance of life, and drug-induced excessive changes in blood pressure or arrhythmias can lead to lethal changes. Thus, non-clinical testing in drug development includes detailed evaluation of effects on systemic hemodynamics and proarrhythmia risk. The general principles and recommendations for these studies are provided in the guideline Safety Pharmacology Studies for Human Pharmaceuticals (ICH S7A). By following this guidance, researchers are able to conduct risk evaluation of a test substance at a consistent level. In addition, the importance of risk assessment for cardiac contractility has recently become recognized.[1,2] Researches are being conducted to develop and standardize assay systems with a higher sensitivity and extrapolatability to humans, including such consortia as the Health and Environmental Science Institute (HESI).[3,4] This new perspective on risk requires the continuous development of evaluation systems.

Comprehensive cardiovascular risk assessment can be performed using animals or isolated Langendorff hearts, specifically regarding proarrhythmia and cardiac contractility.[5] From the viewpoint of animal welfare, however, cell culture assay would be more desirable as an alternative *in vitro* system. The discovery of induced pluripotent stem cells (iPSCs) and subsequent establishment of human iPSC-derived cardiomyocytes (CMs) (hiPSC-CMs) have produced promising tools.[6] Using the hiPSC-CMs, development of an *in vitro* assay system to detect functional changes in CMs has been attempted.[7–9] The establishment of assay systems will enable accurate prediction of drug effects in humans without using experimental animals.

Most studies using hiPSC-CMs have been conducted in two-dimensional (2D) monolayer cultures consisting of CMs. Monolayer cultures are simply planar aggregations of CMs and are therefore considered to substantially differ from native myocardial tissue. The majority of cardiac tissue volume consists of CMs, and the remaining non-myocytes are predominantly vascular endothelial cells, followed by cardiac fibroblasts. The interaction between CMs and non-myocytes also plays an important role in maintaining cardiac structure and function.[10] Taken together, there is a concern that the sensitivity of cell-based assays to detect drug-induced responses is lower in a monolayer culture composed only of CMs. Indeed, monolayer cultures of hiPSC-CMs are used for the assessment of cardiotoxicity including proarrhythmia,[11–13] although the effects of some compounds cannot be detected accurately. In particular, with regard to contractile force, the power to detect drug-induced

Received 13 November 2020; accepted 14 May 2021;
https://doi.org/10.1016/j.omtm.2021.05.007.

Correspondence: Kiyoshi Tadano, Drug Safety Research Labs, Astellas Pharma Inc., Tsukuba, Ibaraki 305-8585, Japan.
E-mail: kiyoshi.tadano@astellas.com

inotropic effects is limited.[14–16] Recently, successful attempts have been made in evaluating cardiac contractility under refined conditions in a 2D model.[17] However, the index of inotropy was not still detected when pixel displacement was used as a surrogate of contractility. The reason is that hiPSC-CMs are considered to be immature, and it is necessary to construct a model that can quantify the changes in contractile force. Various approaches to improve the maturity of hiPSC-CMs, including long-term culture, electrical pacing, and co-culture with non-CMs, have been attempted.[18,19] Furthermore, the generation of three-dimensional (3D) cardiac tissues has also been developed,[6] and combination with different approaches was used to improve the maturity.[17,20] However, the method to generate matured cardiac tissues is complex and needs a long culture period.

We previously developed a convenient method to generate 3D tissue constructs in a short culture period by coating the cell surface with extracellular matrix (ECM) proteins. Our previous studies have shown the possibility that 3D cardiac tissue consisting of CMs can detect drug-induced changes in contractility with a cell motion imaging system.[21] Furthermore, cardiac tissues containing fibroblasts were more potent in the contraction than those consisting of CMs,[22] and thus co-culture with fibroblasts was expected to mimic the behavior of living tissues. We hypothesized that the convenient cardiac tissue created by co-culture with non-CMs could be used for simultaneous evaluation of drug-induced repolarization and contractility by imaging analysis. The present study was carried out with the aim of achieving both improvement of the power to detect and high versatility.

RESULTS

Structure and motion behavior of the 3D cardiac tissues

Immunofluorescence imaging of cardiac troponin T (cTnT) for CMs, vimentin for fibroblasts, and CD31 for endothelial cells was performed to confirm the cell types that constituted the cardiac tissue (Figures 1A and 1B). In order to characterize the morphology and architecture of hiPSC-derived 3D cardiac tissues, cardiac structural markers (α-actinin, ventricular myosin light chain [MLC2v], arterial myosin light chain 2 [MLC2a], and connexin43) (Figures 1C and 1D) and ECMs (fibronectin [FN], laminin, collagen type I) (Figures 1E–1G) were used. CMs in the cardiac tissues were characterized by the typical sarcomere structure of α-actinin and predominant expression of the ventricular-specific isoform MLC2v. The formation of gap junctions was confirmed from the expression of connexin43. Furthermore, matrix proteins such as FN, laminin, and collagen type I were expressed in the cardiac tissues. The formation of vascular networks was confirmed by staining appearance with CD31 antibody. The cardiac tissues showed synchronized and spontaneous beating. Baseline beating rate (BR) was 29.0 ± 8.7 beats/min (n = 72), and baseline values of contractile and relaxation parameters were 29.1 ± 9.1 μm/s for maximum contraction speed (MCS), 21.1 ± 8.0 μm/s for maximum relaxation speed (MRS), 3.20 ± 1.08 μm for contraction deformation distance (CDD), 3.09 ± 1.20 μm for relaxation deformation distance (RDD), and 6.28 ± 2.26 μm for average deformation distance (ADD) and those of repolarization parameters were 0.26 ± 0.02 s for contraction time (CT), 0.38 ± 0.04 s for relaxation time (RT), and 0.64 ± 0.05 s for contraction-relaxation duration (CRD) (Figure 2).

Effects of vehicle on motion waveform and parameters

A representative contraction and relaxation waveform before and after 4 treatments with dimethyl sulfoxide (DMSO) is shown in Figure 3A. The percentage change compared to medium-treated values (baseline values) after the addition of 0.03% DMSO up to 4 times was calculated. During vehicle treatment, there were no statistically significant changes in any parameter (Figure 3B). The value of the percentage of baseline with two standard deviations (SDs) after treatment with DMSO was determined as background range and used as criteria for evaluating the effects of test compounds. Background range was determined to be the mean ± 2 SD value, that is, 70%–130% for BR and MRS, 75%–125% for MCS, CDD, RDD, and ADD, and 95%–105% for CT, RT, and CRD.

Effects of test compounds on contraction and relaxation waveform

Representative contraction and relaxation waveforms before and after treatment with test compounds are shown in Figure 4. Among 6 positive inotropic drugs (isoproterenol, dobutamine, milrinone, ouabain, pimobendan, and glibenclamide), all compounds except dobutamine and glibenclamide increased maximum speed of contraction and/or relaxation. Dobutamine decreased only maximum speed of relaxation without altering contraction speed. Glibenclamide did not affect either the contraction or relaxation waveform at all concentrations. The negative inotropic drugs verapamil and flecainide reduced maximum speed of contraction and relaxation. Among test compounds known to cause repolarization delay, E-4031 and flecainide caused prolongation of RT in a concentration-dependent manner and occurrence of arrhythmia-like waves, as shown in a relatively small peak following the relaxation peak. Chromanol 293B slightly prolonged RT at the highest concentration tested. The incidence of arrhythmia-like waves and beating arrest is summarized in Table 1. Isoproterenol and ouabain produced beating arrest at higher concentrations.

Effects of test compounds affecting cardiac contractility or repolarization on the motion parameters

Beating rate

The concentration response of BR is shown in Figure 5. Isoproterenol produced a concentration-dependent increase in BR at 1–30 nM (maximum increase: 164% ± 37% of baseline at 30 nM, $p < 0.01$) and a plateau at 30–1,000 nM. Dobutamine significantly increased BR at all concentrations (171% ± 12% of baseline at 3 μM, $p < 0.01$), but the magnitude of the change was attenuated in a concentration-dependent manner (131% ± 11% of baseline at 100 μM, $p < 0.01$). Ouabain increased BR at 300 nM (130% ± 38% of baseline), although without statistical significance. Verapamil significantly increased BR at the highest concentration of 100 nM (135% ± 32% of baseline, $p < 0.01$). Chromanol 293B significantly increased BR at 30 μM (117% ± 15% of baseline), but this was not considered to

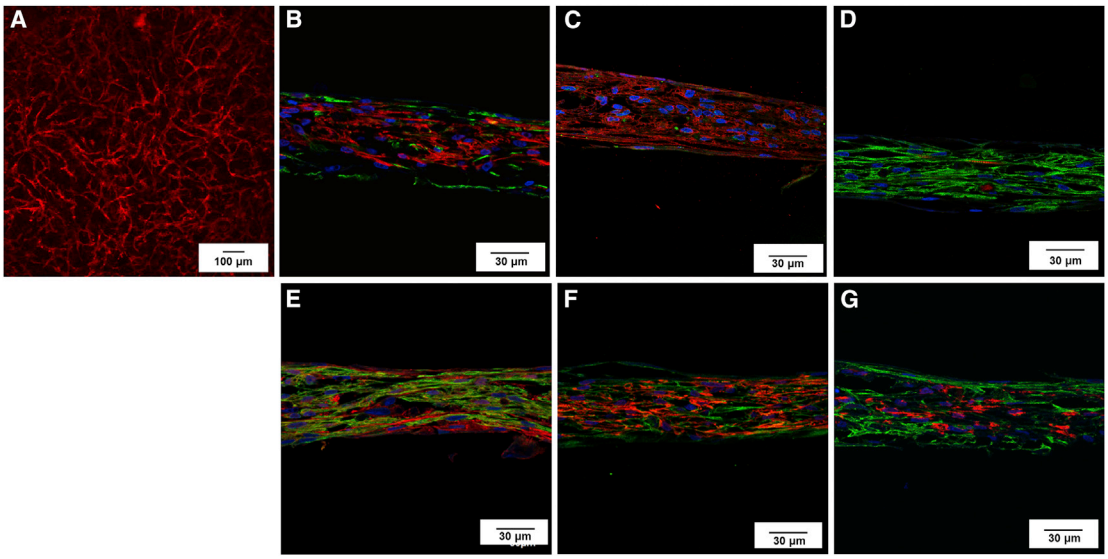

Figure 1. Immunostaining of hiPSC-derived 3D cardiac tissues

Cardiac cell type (A) CD31 (red), (B) vimentin (green) and cardiac troponin T (red), cardiac-specific structural proteins: (C) sarcomeric α-actinin (red) and connexin43 (green), (D) MLC2v (green) and MLC2a (red), and extracellular matrix proteins: (E) fibronectin (red) and cardiac troponin T (green), (F) laminin (green) and cardiac troponin T (red), (G) collagen type I (green) and cardiac troponin T (red). Nuclei were stained with DAPI. The fluorescent images were acquired at 10 (A) or 60 (B–G) magnifications.

be test compound related since the magnitude of the changes was slight.

Contractile and relaxation parameters

Most of the positive and negative inotropic drugs affected contractile or relaxation parameters (Figure 6). Ouabain caused a statistically significant increase in MCS at 300 nM (138% ± 22% of baseline, $p < 0.01$) but decreased MRS at 30–300 nM (61% ± 8% of baseline at 300 nM, $p < 0.01$). Dobutamine caused a statistically significant decrease in MRS at 3–100 µM (58% ± 33% of baseline at 30 µM, $p < 0.01$). Compared to the mean value of the percentage of baseline after treatment with DMSO with two SDs, the following changes were observed. Isoproterenol increased MCS and MRS at 100 nM and above (126% ± 23% and 126% ± 25% of baseline for MCS, 139% ± 33% of baseline for MRS). Milrinone increased MRS at 100 µM and ADD at 3 µM and over (138% ± 43% of baseline for MRS, 144% ± 52% of baseline for ADD). Pimobendan increased ADD at 3 µM (132% ± 31% of baseline). Glibenclamide did not increase MCS, MRS, or ADD at the concentrations tested. Verapamil significantly decreased MCS, ADD, and MRS at 100 nM (61% ± 18%, 67% ± 21%, and 61% ± 22% of baseline, respectively, $p < 0.5$ or $p < 0.01$). Flecainide did not affect MCS, MRS, or ADD in concentrations up to 1 µM, but decreases in MRS and ADD exceeding the baseline levels were observed in some wells. MRS was reduced to 51%–59% of baseline at 300 nM (3 of 6 wells) and to 38% of baseline at 1,000 nM (1 of 6 wells, of which 4 wells were excluded from evaluation because of the appearance of arrhythmia-like waves). ADD was reduced to 71% and 73% of baseline in 2 of 6 wells at 300 nM.

Among test compounds known to cause repolarization delay, E-4031 significantly decreased MRS (71% ± 17% of baseline at 10 nM, $p < 0.01$) without affecting MCS at concentrations of 3 and 10 nM. In chromanol 293B, significantly low values were seen in MCS at 10 µM and over (88% ± 4% of baseline at 10 µM, $p < 0.01$) but were not considered test compound related since the magnitude of the changes was slight.

Repolarization parameters

All test compounds known to cause delayed repolarization prolonged both RT and CRD (Figure 7). E-4031 significantly prolonged RT and CRD at 10 nM and over (158% ± 5% of baseline for RT and 133% ± 4% of baseline for CRD at 30 nM, $p < 0.01$). Flecainide significantly prolonged RT and CRD at 300 nM and over (124% ± 5% of baseline for RT and 118% ± 3% of baseline for CRD at 300 nM, $p < 0.01$). Chromanol 293B produced a slight but significant prolongation of RT and CRD at the highest concentration of 30 µM (115% ± 6% of baseline for RT and 112% ± 3% of baseline for CRD at 30 µM). Statistically significant shortenings of RT and CRD were observed at 30 and/or 100 nM of verapamil (76% ± 7% of baseline for RT and 78% ± 9% of baseline for CRD at 100 nM, $p < 0.01$).

Among other compounds, there were statistically significant prolongations of RT and CRD for dobutamine at the highest concentration of 100 nM (120% ± 3% of baseline for RT, 112% ± 3% of baseline for CRD, $p < 0.01$), for ouabain at 300 nM (131% ± 9% of baseline for RT, 117% ± 7% of baseline for CRD, $p < 0.01$), and for glibenclamide at 10 µM and over (114% ± 11% of baseline at 30 µM for RT, $p < 0.5$; 112% ± 7% of baseline at 30 µM for CRD, $p < 0.01$). A statistically significant shortening of CRD was observed at all concentrations of isoproterenol tested (77% ± 3% or 77% ± 4% of baseline at 30–300 nM, $p < 0.01$), at lower concentrations of dobutamine, 3 and

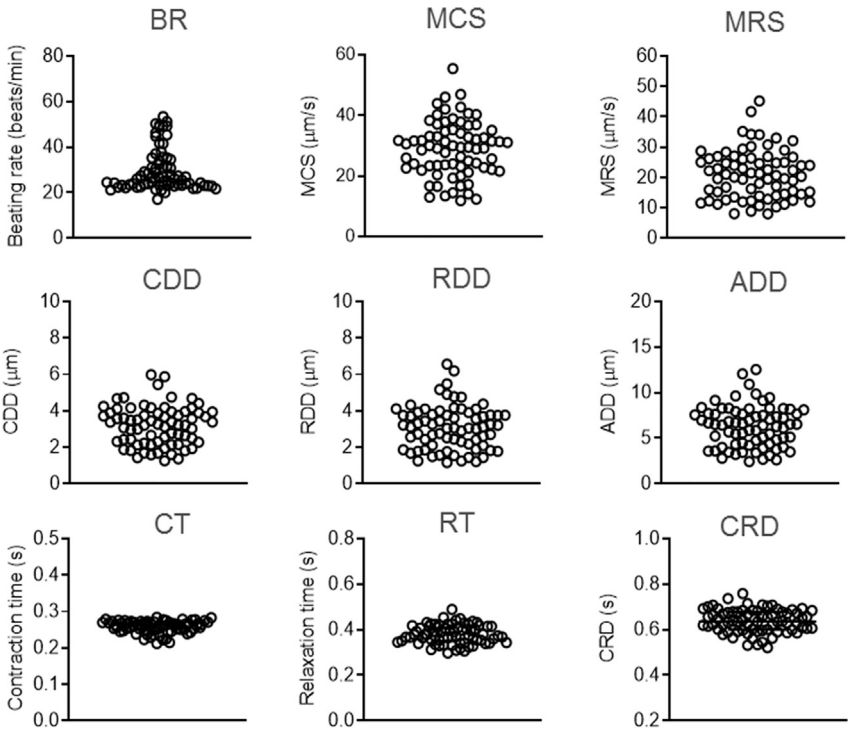

Figure 2. Baseline values of motion parameters acquired with motion vector analysis

All individual values before treatment with test compounds or vehicle were plotted for each parameter. Bar and error bars indicate the mean ± SD (n = 72).

10 μM (86% ± 3% of baseline at 3 μM, $p < 0.01$), and at the lowest concertation of ouabain, 30 nM (93% ± 5% of baseline at 30 nM, $p < 0.5$). Similar to changes in CRD, a shortening of RT was noted for isoproterenol and dobutamine.

DISCUSSION

Since the constructed 3D cardiac tissue has a capillary-like network and expresses both myocardial structural proteins such as α-actinin and MLC2v and ECM proteins, it was confirmed to be similar to the properties of the native tissue. No effects on repolarization and contractile parameters were observed with repeated application of DMSO, indicating a functionally stable system in a steady state. In addition to typical drugs (E-4031, flecainide, and chromanol 293B), which prolong the action potential duration (APD) of CMs, dobutamine, ouabain, and glibenclamide caused prolongation of RT and CRD. Moreover, E-4031 and flecainide also induced arrhythmia-like waveforms, which were considered due to excessive prolongation of repolarization. Verapamil, which shortens APD, shortened both RT and CRD. These results are generally consistent with findings in a microelectrode array assay system in monolayers of hiPSC-CMs and an human ether-a-go-go-related gene (HERG) channel assay.[12,23,24] We have therefore demonstrated that this 3D assay system can be used to evaluate the effects of drugs on myocardial repolarization, as with a monolayer culture.

Next, to investigate the effects on cardiac contractility, we tested 6 compounds with positive inotropic effects in human or Langendorff-perfused hearts. These compounds enhance myocardial contraction by increasing intracellular Ca^{2+} concentration through different mechanisms or by enhancing Ca^{2+} sensitivity. Among the compounds tested, 4 drugs (isoproterenol, milrinone, ouabain, and pimobendan) increased MCS, MRS, or ADD as indices of contractility, suggesting the possibility to detect drug-induced effects on contractility irrespective of the pharmacological mechanisms of action. The present results are consistent with the finding that accuracy ranged from 50% to 75% in a blinded multicenter study using 8 positive inotropic drugs in hiPSC-derived engineered heart tissue (EHT).[17] In the future, the usefulness of this test system will be further clarified by testing more compounds.

The results described so far have shown the usefulness of our 3D cardiac tissue for the evaluation of cardiotoxicity; however, they also raised several issues. One issue is that increases in contractility by dobutamine and glibenclamide were not observed. Dobutamine acts on adrenergic receptors, and the positive inotropic effect occurs primary via the same β1 receptor stimulation as isoproterenol. In contrast to our results, Saleem et al.[17] reported an increase in the contractility of cardiac tissues when dobutamine was added. Since α-adrenergic receptors have been reported to produce negative inotropic effects in cultured CMs,[25] the effects mediated by α-adrenergic receptors might mask the positive inotropic effects of β-adrenergic receptors. The altered balance of receptor subtypes in 3D cardiac tissue might produce effects on contractility different from those in adult heart. Glibenclamide is another drug that did not produce the expected effects on contractility. It was categorized as positive inotropy based on results in Langendorff-perfused hearts of rabbits,[26] but the effects on the 3D cardiac tissues reported by others were controversial.[14,17] Few reports have investigated the effects on cardiac contractility in humans, and thus it is unclear whether the present results mimic biological responses in humans.

In the cases of milrinone and pimobendan, there were dissociations between concentrations at which the positive inotropic effect was observed in 3D cardiac tissues and clinical study or Langendorff-perfused heart. These findings suggest low expression of receptors or enzymes associated with the regulation of contractility compared to adult cardiac tissue. The concentrations required to cause an increase in contractility by these drugs were 100–350 times and 3,000 times higher than those required in humans or Langendorff-perfused hearts of guinea pigs, respectively.[2,27] A relatively higher concentration of milrinone was also required to increase contractility in a 3D cardiac tissue reported by Saleem et al.,[17] whereas the EHT subjected to 10-week electrical field stimulation increased

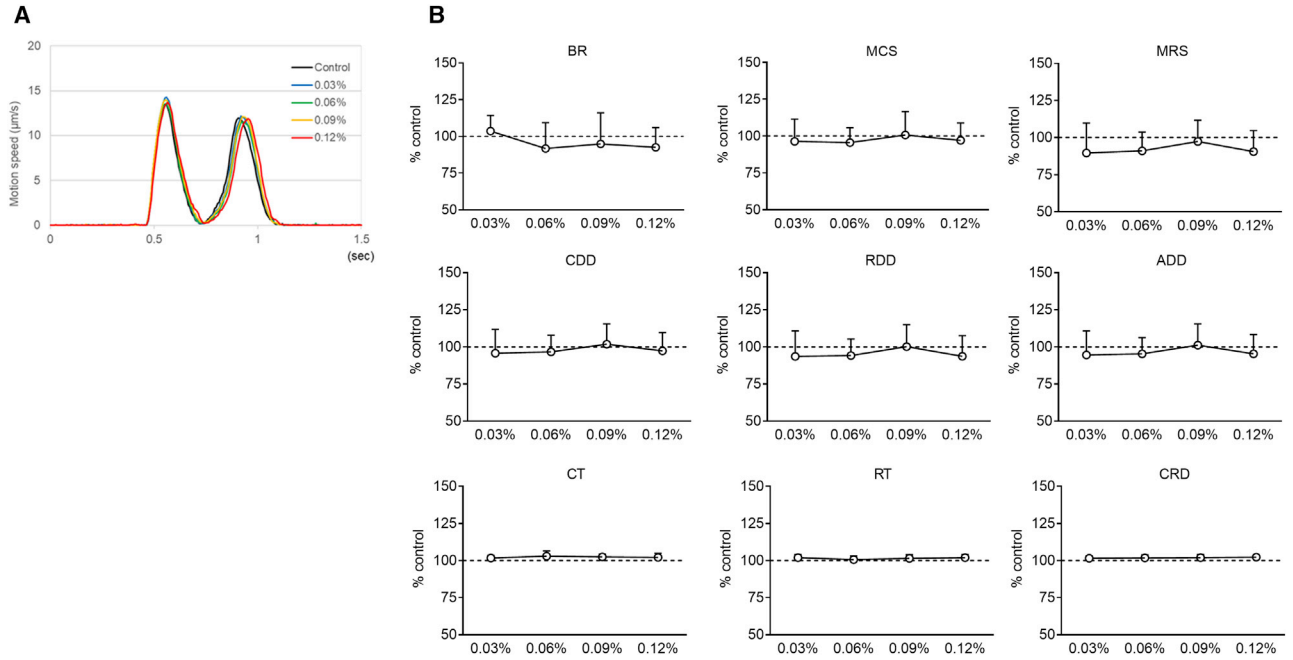

Figure 3. Effects of DMSO on contraction and relaxation waveform

(A) Examples of a typical motion waveform are represented before (baseline) and after four times treatment with 0.03% DMSO in hiPSC-derived 3D cardiac tissues. (B) Effects of 0.03% DMSO on motion parameters acquired from motion vector analysis. The values are represented as mean ± SD (n = 6) of the percentage of baseline after treatment with DMSO compared to medium-treated values.

contractility at effective therapeutic plasma concentrations (ETPCs). Since these results suggest the possibility that drug responsiveness is associated with the maturation of cardiac tissue, the low potency for contractile effect of some drugs may be associated with the immaturity of 3D cardiac tissue. This is also suggested by the report that the expression of phosphodiesterase 3A (PDE3A), which is a target molecule of milrinone, was lower in the spheroids consisting of CMs than the adult left ventricle and that a positive inotropic effect was not observed.[28] On the other hand, the positive inotropic effect of pimobendan was observed in common at higher concentrations than the ETPC in other cardiac tissue models,[17,20] and thus it might be caused by high tissue permeability of the drug, as discussed by Qu et al.[20] As another possible reason, since fetal bovine serum (FBS) was contained in the medium, it cannot be ruled out the possibility that the lower sensitivity is likely due to the protein binding for some compounds.[29] A second issue is that the degree of contractile response by some compounds differed among wells. This is partly considered due to variations in baseline values among wells. For example, an increase in ADD by pimobendan was noted only in wells with relatively low values before treatment (K. Tadano, unpublished data). Possible causes of such variation might include differences in the differentiation induction efficiency of iPSCs into CMs (lot-to-lot variation) or in structural heterogeneity in preparing multilayers. Differentiation efficiency might be improved by methods to generate ventricular-type CMs from iPSCs or to obtain high-purity CMs using microRNA.[30,31] Structural heterogeneity may be improved by controlling cardiomyocyte polarity using nanofibers and by aligning orientation of the myocardial contraction constant.[32]

The 3D cardiac tissue consisting of CMs, cardiac fibroblasts, and cardiac microvascular endothelial cells used in the present study is a highly convenient model system that can mimic the tissue structure of the living body in the same culture period as 2D culture without complicated procedures. A detailed investigation of pharmacological effects in this unique 3D cardiac tissue showed not only changes in repolarization caused by cardiac ion channel blockers such as HERG channel but also changes in contractility mediated by multiple mechanisms of action. In the present study, the effects of some drugs with a positive inotropic effect could not be evaluated qualitatively and quantitatively. One of the reasons was probably the immaturity of the cardiac tissue. However, since our findings using 3D cardiac tissue were similar to previous results reported in the literature, this assay system will become one of the useful tools for cardiotoxicity by refinement of the conditions.

MATERIALS AND METHODS

Preparation of CMs

Human iPSCs (253G1) were obtained from the Riken BioResource Research Center (253G1; Ibaraki, Japan).[33] They were cultured on a mitomycin C-treated mouse embryonic fibroblast feeder cell (Millipore Co., Bedford, MA, USA) layer in KnockOut Serum Replacement (KSR)-based medium (Thermo Fisher Scientific, Waltham, MA, USA) to which 4 ng/mL fibroblast growth factor (FGF)-2

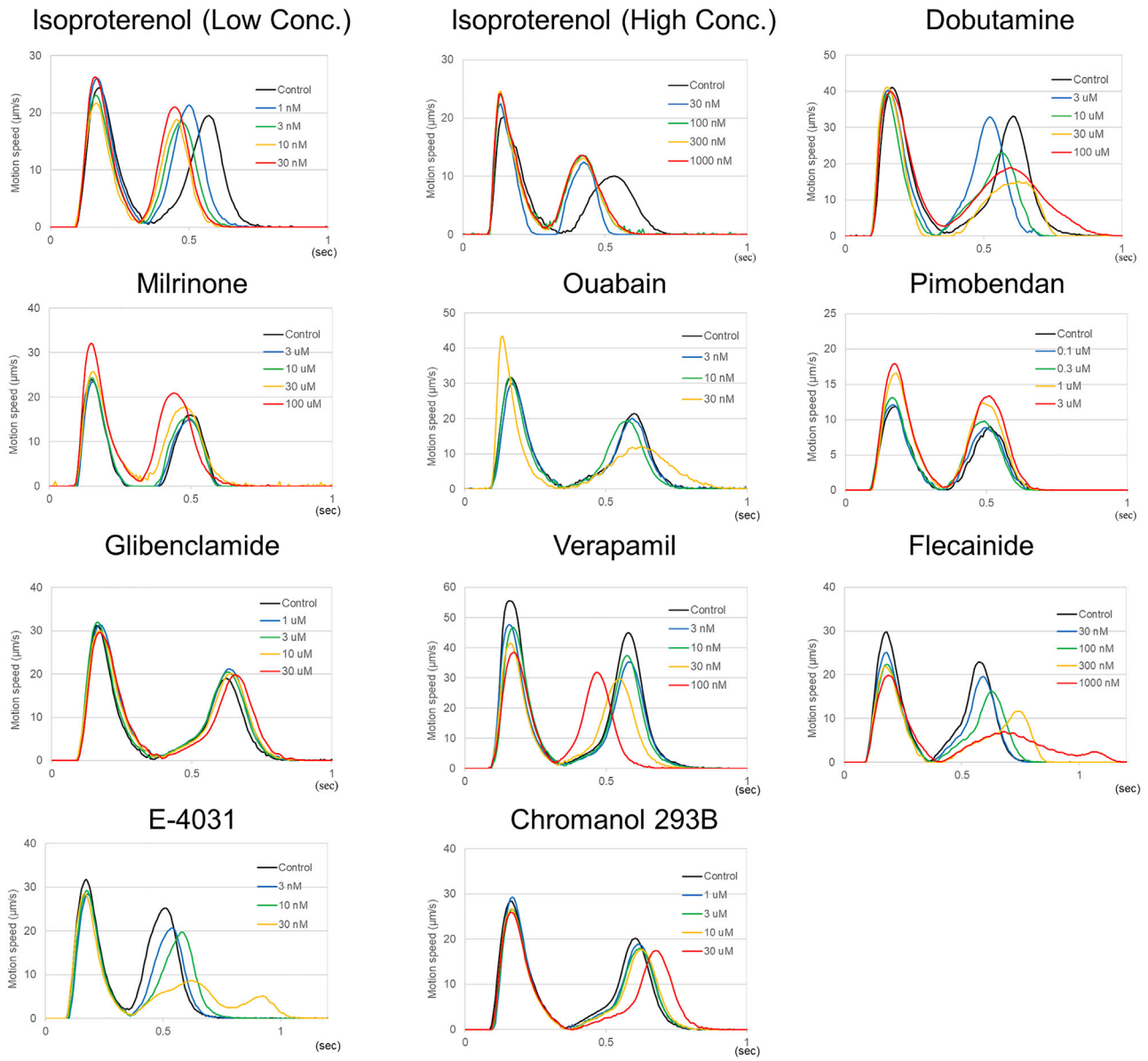

Figure 4. Effects of test compounds on contraction and relaxation waveform

Representative examples of motion waveforms are represented before (baseline) and after treatment with isoproterenol (1–30 nM or 30–1,000 nM), dobutamine (3–100 μM), milrinone (3–100 μM), ouabain (3–30 nM), pimobendan (0.1–3 μM), glibenclamide (1–30 μM), verapamil (3–100 nM), flecainide (30–1,000 nM), E-4031 (3–30 nM), and chromanol 293B (1–30 μM) in hiPSC-derived 3D cardiac tissues.

(Sigma-Aldrich, St. Louis, MO, USA) was added. KSR-based medium consisted of knockout-Dulbecco's modified Eagle's medium (DMEM)/F12 medium (Thermo Fisher Scientific) to which 20% v/v KSR, 0.1 mM 2-mercaptoethanol (Thermo Fisher Scientific), minimum essential medium (MEM) with nonessential amino acids (Thermo Fisher Scientific), and 2 mM L-glutamine (Thermo Fisher Scientific) were added. hiPSCs were passaged every 7 days as small clumps by treatment with 1 mg/mL dispase II (Sigma-Aldrich), followed by pipetting.

The conditions for differentiation of hiPSCs to hiPSC-CMs were modified from a method previously reported by Sasano et al.[33] Briefly, hiPSCs were collected as small clumps by Accutase (Innovative Cell Technologies, San Diego, CA, USA) treatment and then pipetted and strained with a 100-μm cell strainer (Corning, New York, NY, USA). The hiPSC clumps were then suspended in 30 mL of complete StemPro-34 medium (Thermo Fisher Scientific) including 50 μg/mL L-ascorbic acid 2-phosphate trisodium salt (FUJIFILM Wako Pure Chemical, Osaka, Japan), 2 mM L-glutamine, and 400 μM

Table 1. Incidence of arrhythmia-like wave and beating arrest

	Arrhythmia-like wave		Beating arrest	
Compounds	Incidence	Concentration (nM)	Incidence	Concentration (nM)
Isoproterenol	0/6	–	1/6	300
			1/6	1,000
Dobutamine	0/6	–	0/6	–
Milrinone	0/6	–	0/6	–
Ouabain	0/6	–	2/6	300
			6/6	1,000
Pimobendan	0/6	–	0/6	–
Glibenclamide	0/6	–	0/6	–
Flecainide	4/6	1,000	0/6	–
Verapamil	0/6	–	0/6	–
E-4031	3/6	30	0/6	–
	6/6	100		
Chromanol 293B	0/6	–	0/6	–

1-thioglycerol (Sigma-Aldrich). Differentiation was induced by adding 10 μM Y-27632 (FUJIFILM Wako Pure Chemical.), 10 ng/mL bone morphogenetic protein (BMP)-4 (R&D Systems, Minneapolis, MN, USA), 5 ng/mL FGF-2, and 6 ng/mL activin A (R&D Systems).

Cell suspensions were seeded into a 30-mL single-use bioreactor (ABLE & Biott, Tokyo, Japan) at 37°C and agitated at a rate of 55 rpm. The culture medium was exchanged containing 10 ng/mL BMP-4, 5 ng/mL FGF-2, and 6 ng/mL activin A on Day 2; 4 μM IWR-1-endo (FUJIFILM Wako Pure Chemical) and 10 μM IWP-2 (Tocris Bioscience, Minneapolis, MN) on Days 3 and 5; after Days 11, 5 ng/mL VEGF165 (Humanzyme, Chicago, IL, USA) and 10 ng/mL FGF-2 on Days 6, 8, 10, and 12. On Day 13, hiPSC-CMs were dissociated from spheroids into single-cell suspensions by Accumax (Innovative Cell Technologies) treatment and disrupted through repeated pipetting and a 40-μm cell strainer (Corning). Single cells of hiPSC-CMs were then suspended in DMEM (Nacalai Tesque, Kyoto, Japan) with 10% FBS (Thermo Fischer Scientific) and antibiotic-antimycotic mixed stock solution (Nacalai Tesque).

Preparation of fibroblasts or vascular endothelial cells

Normal human cardiac fibroblasts (NHCFs; passage 6) and human cardiac microvascular endothelial cells (HMVECs; passage 6–7) obtained from Lonza (Allendale, NJ, USA) were used in the experiments. After culture in fibroblast growth medium (FGM-3, Lonza), NHCFs were dissociated with 0.1% trypsin (FUJIFILM Wako Pure Chemical) and centrifuged for 5 min at 160 × *g*. After the supernatant was removed, the cells were suspended in phosphate-buffered saline (PBS) (Nacalai Tesque) and used in the layer-by-layer approach described below. HMVECs were cultured in endothelial growth medium (EGM-2, Lonza) and then dissociated with 0.25% trypsin-EDTA and centrifuged for 5 min at 160 × *g*. After the supernatant was removed, the cells were suspended in EGM-2 and used for tissue construction without the layer-by-layer approach.

Construction of 3D cardiac tissues

As reported previously by Amano et al.,[22] hiPSC-CMs and NHCFs were coated with nanofilms of FN and gelatin (G) on each cell surface with a filtration-based layer-by-layer approach. In brief, each suspension of hiPSC-CMs and NHCFs was added into a 24-mm Transwell with a 3-μm pore size (Corning) and immersed in 0.2 mg/mL FN (Sigma-Aldrich) for 1 min at 500 rpm with a shaking incubator (SI-300, AS ONE, Osaka, Japan). The cell suspension was shaken to remove the solution, and the coated cells were then washed with PBS. Next, the cells were immersed in 0.2 mg/mL G (FUJIFILM Wako Pure Chemical) and washed with PBS in the same manner as FN. After four repetitions of this cycle, they were again immersed in FN solution and washed with PBS. The coated hiPSC-CMs and NHCFs were suspended in DMEM (Nacalai Tesque).

To construct a multilayer tissue containing blood capillary networks, hiPSC-CMs and NHCFs coated with FN/G nanofilms were co-cultured with uncoated HMVECs (cell number ratio: CM75:NHCF25:HMVEC10). The mixture of cell suspensions consisting of coated hiPSC-CMs (0.75×10^6 cells), NHCFs (0.25×10^6 cells), and uncoated HMVECs (1.0×10^5 cells) in DMEM containing 10% FBS (Life Technologies, Carlsbad, CA) was seeded into a 6.5-mm Transwell with a 0.4-μm pore size (Corning) that was precoated with FN. DMEM was then added into the outside of the Transwell until the bottom of the insert was fulfilled. After incubation for 2 h at 37°C in 5% CO_2, further medium was added into the outside of the Transwell so that the inside and outside of the Transwell were filled with medium. The 3D cardiac tissues were incubated for 6–8 days, with half of the medium from the outside of the Transwell replaced daily.

Immunofluorescence staining

Cardiac tissues were fixed with 4% paraformaldehyde (Nacalai Tesque). Experiments were performed on paraffin sections after antigen retrieval

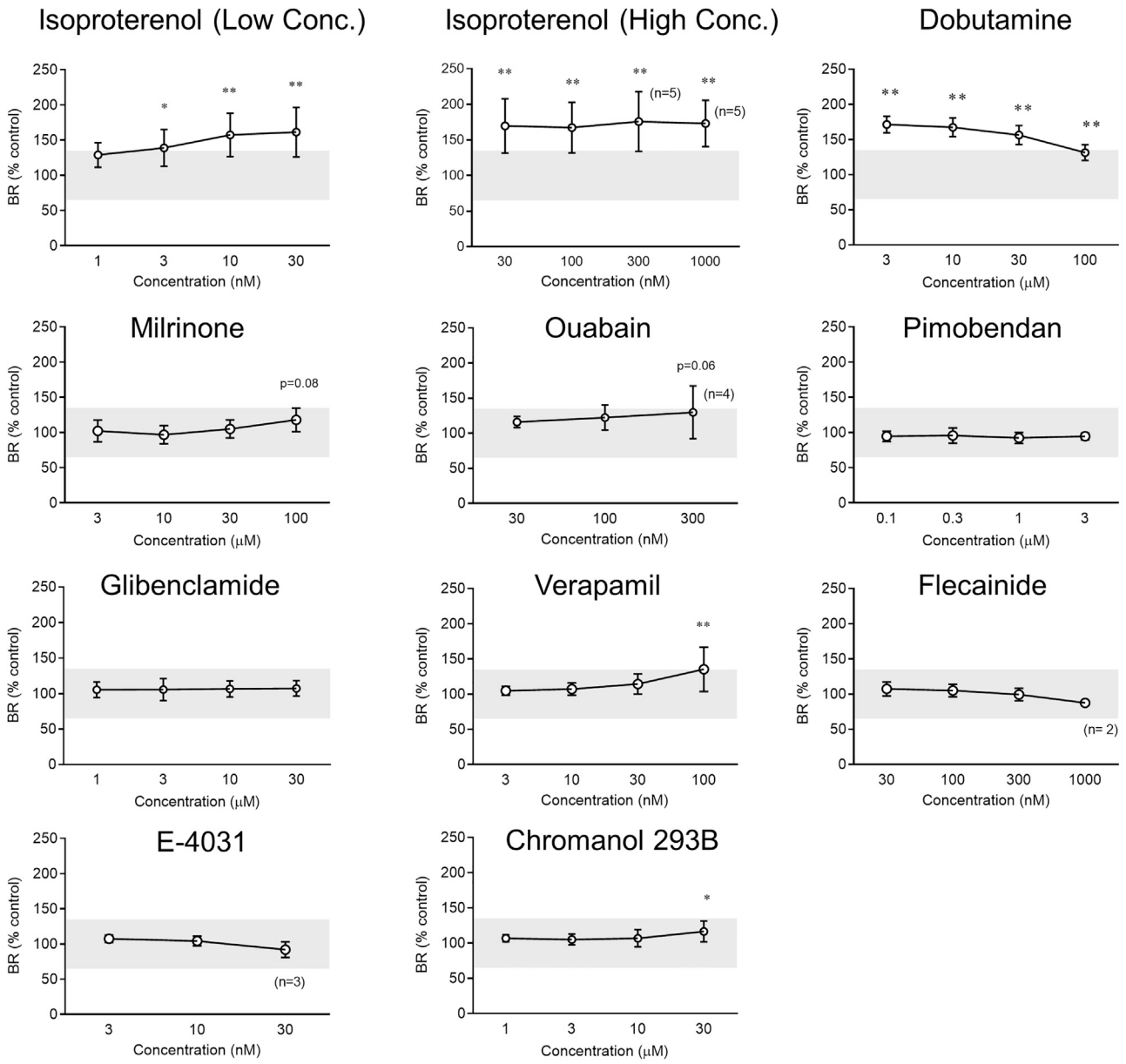

Figure 5. Effects on beating rate of test compounds affecting cardiac contractility and repolarization

Data are expressed as means ± SD of 6 preparations. *p < 0.05, **p < 0.01 compared with baseline (one-way ANOVA followed by Dunnett post hoc test). The gray shaded area shows mean and 2 SD of percentage of baseline after treatment with vehicle.

with citrate buffer (pH 6.0) at 121°C for 20 min. The tissues were incubated with primary antibodies including mouse or rabbit anti-cTnT (1:200 dilution; Abcam, Cambridge, UK), rabbit anti-vimentin (1:200, Abcam), mouse anti-sarcomeric α-actinin (1:400; Sigma-Aldrich), rabbit anti-connexin43 (1:100; Abcam), mouse anti-MLC2a (1:100; Synaptic Systems, Goettingen, Germany), rabbit anti-MLC2v (1:200; Proteintech, Rosemont, IL, USA), mouse anti-FN (1:200; Abcam), rabbit anti-laminin (1:30; Sigma-Aldrich), and rabbit anti-collagen type I (1:500; Abcam). The endothelial cells were immunostained with mouse anti-CD31 antibody (1:200; Dako, Glostrup, Denmark). The tissues were permeabilized with 0.2% Triton X (Sigma-Aldrich), and then non-specific reactivity was blocked with 1% BSA. The tissues were labeled by primary antibodies. Secondary antibodies (1:200) such as Alexa Fluor 488- or Alexa Fluor 546-conjugated goat anti-mouse or anti-rabbit IgG (H+L) (Thermo Fisher Scientific) were added to the tissues. Nuclei were stained with 4′,6-diamidino-2-phenylindole (DAPI) (Life Technologies) and observed by confocal laser scanning microscopy (FLUOVIEW FV10i; Olympus, Tokyo, Japan).

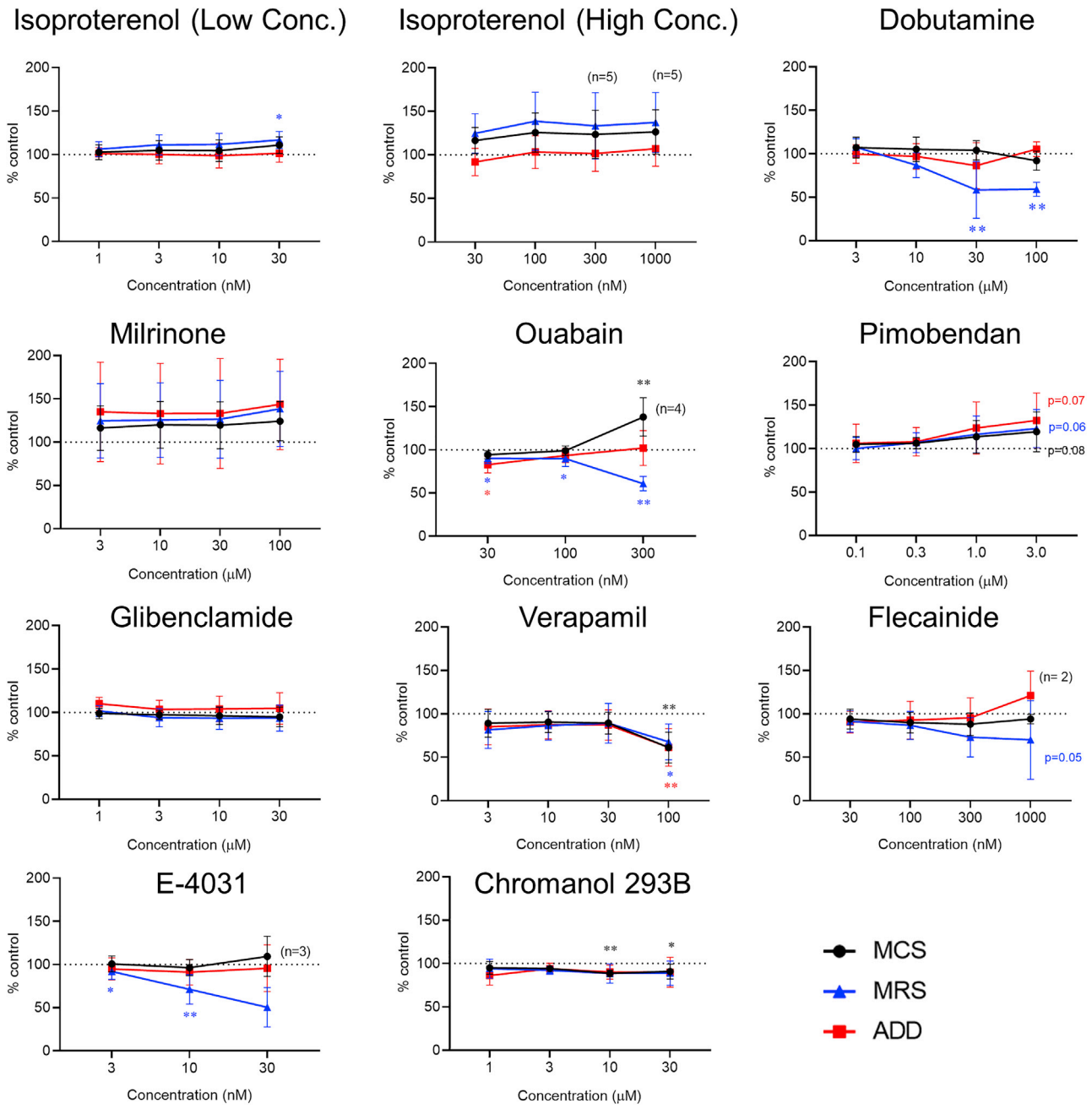

Figure 6. Effects on contractile and relaxation parameters of test compounds

Maximum contraction speed, black, closed circle; maximum relaxation speed, blue, closed triangle; average deformation distance, red, closed square. Data are expressed as means ± SD of 6 preparations. *p < 0.05, **p < 0.01 compared with baseline (one-way ANOVA followed by Dunnett post hoc test).

Drugs

Ten test compounds were assayed in this study, namely, isoproterenol and dobutamine (adrenergic β1 agonists), milrinone (PDE3 inhibitor), ouabain (Na^+-K^+ ATPase inhibitor), pimobendan (Ca^{2+} sensitizer), glibenclamide (sulfonylurea drug), flecainide (Na^+ channel blocker), verapamil (Ca^{2+} channel blocker), E-4031 (HERG channel blocker), and chromanol 293B (slow voltage-gated potassium channel (I_{Ks}) channel blocker). Milrinone, E-4031, and verapamil were purchased from FUJIFILM Wako Pure Chemical. Pimobendan was purchased from AK Scientific (Union City, CA, USA). The other compounds were purchased from Sigma-Aldrich. Compounds were dissolved in DMSO (FUJIFILM Wako Pure Chemical) or distilled

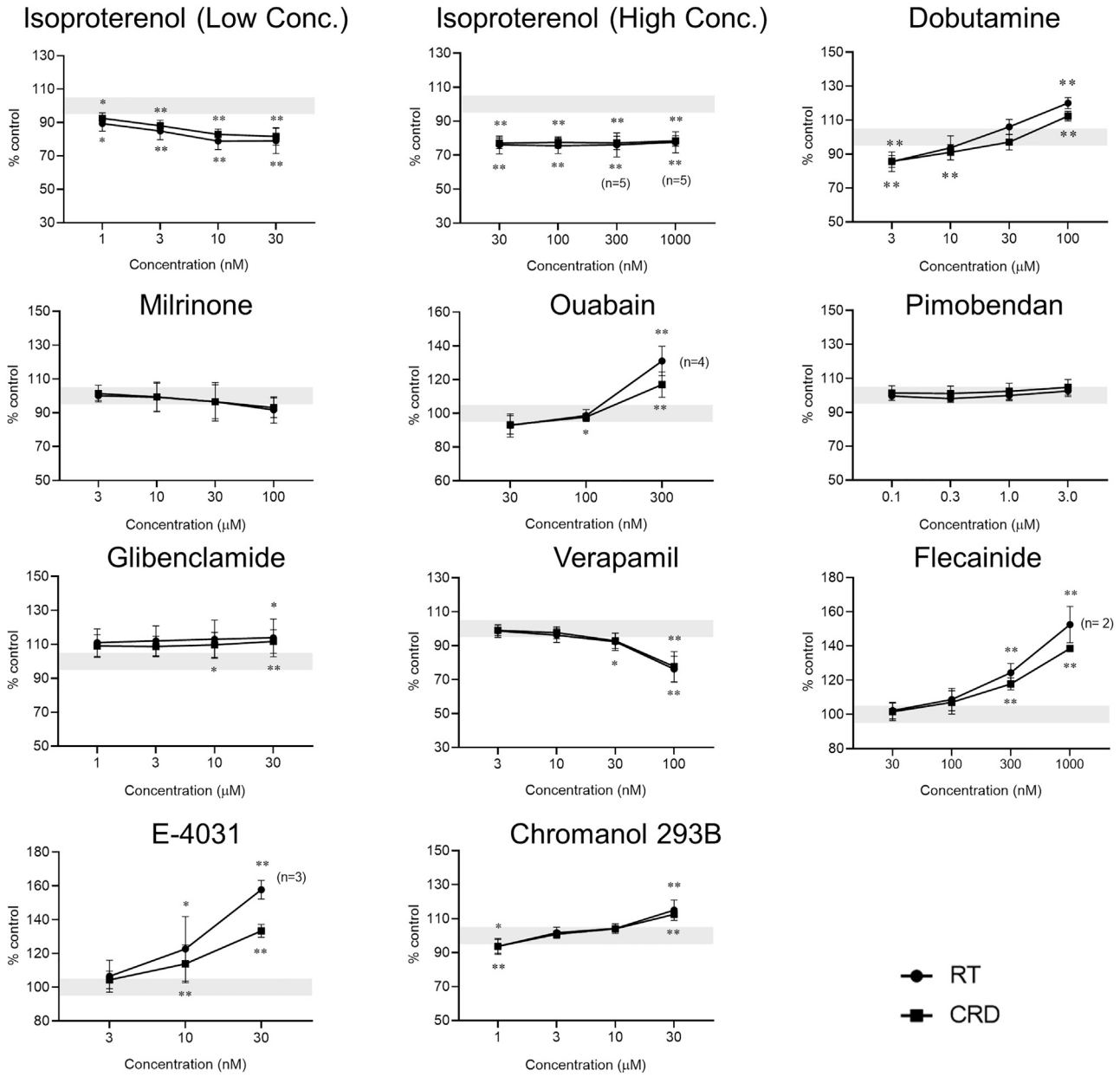

Figure 7. Effects on repolarization parameters of test compounds

Relaxation time, closed circle; contraction-relaxation duration, closed square. Data are expressed as means ± SD of 6 preparations. *p < 0.05, **p < 0.01 compared with baseline (one-way ANOVA followed by Dunnett post hoc test). The gray shaded area shows mean and 2 SD of percentage of baseline after treatment with vehicle.

water (for isoproterenol). The final concentration of each compound in the culture medium was 0.03% v/v. Background ranges were determined by treatment with vehicle alone.

Cell motion analysis

Video images of beating cardiac tissues were recorded as sequential phase-contrast images with a ×10 objective at a frame rate of 150 frames/s and resolution of 2,048 × 2,048 pixels with an SI8000 cell motion imaging system (Sony, Tokyo, Japan). During stabilization for ∼20 min, video images of each well were recorded three times at intervals of ∼5 min for a duration of 5 s each. After the recording of beating cardiac tissues, the video images were analyzed to obtain the motion vector with SI8000C Analyzer Software (Sony).

The culture medium was applied to obtain a baseline value of each well. Subsequently, test compounds were applied from the lowest to the highest concentration for 20 min each in a cumulative manner. As background data, treatment with vehicle (0.03% DMSO) instead

of test compounds was conducted 4 times in the same manner (final concentration of DMSO after 4th treatment was 0.12%). Video images for analysis were recorded for 10 s from 20 min after treatment with the culture medium or each concentration of test compound. For isoproterenol and dobutamine, images were also recorded at 5 min after treatment because of short-lasting responses. A series of parameters was analyzed from the motion waveforms, namely, MCS, MRS, and ADD as parameters representing the contractile and relaxation property; RT and CRD as parameters representing the repolarization property; and BR. Drug effects were evaluated using the percent change from baseline for each parameter. When arrest or an arrhythmia-like waveform was noted, data at that concentration were excluded from quantitative evaluation.

Data analysis

Data are expressed as the mean ± SD. Statistical analysis was performed with one-way ANOVA followed by Dunnett's multiple comparison test using GraphPad Prism (La Jolla, CA). $p < 0.05$ was considered statistically significant.

ACKNOWLEDGMENTS

We thank Yumi Sasano of Nagase & Co., Ltd for providing hiPSC-CMs and Takami Akagi of the Graduate School of Frontier Biosciences at Osaka University for his expert assistance.

AUTHOR CONTRIBUTIONS

Conceptualization, S.M. and K. Takamatsu; methodology, M.A.; investigation, K. Tadano, Y.T., and M.T.; writing – original draft, K. Tadano; writing – review & editing, S.M., Y.T., K.K., and K. Takamatsu; supervision, Y.S.

DECLARATION OF INTERESTS

The authors declare no competing interests.

REFERENCES

1. Hamlin, R.L., and Del Rio, C. (2010). An approach to the assessment of drug-induced changes in non-electrophysiological properties of cardiovascular function. J. Pharmacol. Toxicol. Methods *62*, 20–29.
2. Wallis, R., Gharanei, M., and Maddock, H. (2015). Predictivity of in vitro non-clinical cardiac contractility assays for inotropic effects in humans–A literature search. J. Pharmacol. Toxicol. Methods *75*, 62–69.
3. Sarazan, R.D., Mittelstadt, S., Guth, B., Koerner, J., Zhang, J., and Pettit, S. (2011). Cardiovascular function in nonclinical drug safety assessment: current issues and opportunities. Int. J. Toxicol. *30*, 272–286.
4. Guth, B.D., Chiang, A.Y., Doyle, J., Engwall, M.J., Guillon, J.M., Hoffmann, P., Koerner, J., Mittelstadt, S., Ottinger, S., Pierson, J.B., et al. (2015). The evaluation of drug-induced changes in cardiac inotropy in dogs: Results from a HESI-sponsored consortium. J. Pharmacol. Toxicol. Methods *75*, 70–90.
5. Guo, L., Dong, Z., and Guthrie, H. (2009). Validation of a guinea pig Langendorff heart model for assessing potential cardiovascular liability of drug candidates. J. Pharmacol. Toxicol. Methods *60*, 130–151.
6. Branco, M.A., Cabral, J.M.S., and Diogo, M.M. (2020). From Human Pluripotent Stem Cells to 3D Cardiac Microtissues: Progress, Applications and Challenges. Bioengineering (Basel) *7*, 92.
7. Cerignoli, F., Charlot, D., Whittaker, R., Ingermanson, R., Gehalot, P., Savchenko, A., Gallacher, D.J., Towart, R., Price, J.H., McDonough, P.M., and Mercola, M. (2012). High throughput measurement of Ca^{2+} dynamics for drug risk assessment in human stem cell-derived cardiomyocytes by kinetic image cytometry. J. Pharmacol. Toxicol. Methods *66*, 246–256.
8. Huo, J., Kamalakar, A., Yang, X., Word, B., Stockbridge, N., Lyn-Cook, B., and Pang, L. (2017). Evaluation of batch variations in induced pluripotent stem cell-derived human cardiomyocytes from 2 major suppliers. Toxicol. Sci. *156*, 25–38.
9. Takasuna, K., Asakura, K., Araki, S., Ando, H., Kazusa, K., Kitaguchi, T., Kunimatsu, T., Suzuki, S., and Miyamoto, N. (2017). Comprehensive in vitro cardiac safety assessment using human stem cell technology: Overview of CSAHi HEART initiative. J. Pharmacol. Toxicol. Methods *83*, 42–54.
10. Souders, C.A., Bowers, S.L.K., and Baudino, T.A. (2009). Cardiac fibroblast: the renaissance cell. Circ. Res. *105*, 1164–1176.
11. Kitaguchi, T., Moriyama, Y., Taniguchi, T., Maeda, S., Ando, H., Uda, T., Otabe, K., Oguchi, M., Shimizu, S., Saito, H., et al. (2017). CSAHi study: Detection of drug-induced ion channel/receptor responses, QT prolongation, and arrhythmia using multi-electrode arrays in combination with human induced pluripotent stem cell-derived cardiomyocytes. J. Pharmacol. Toxicol. Methods *85*, 73–81.
12. Ando, H., Yoshinaga, T., Yamamoto, W., Asakura, K., Uda, T., Taniguchi, T., Ojima, A., Shinkyo, R., Kikuchi, K., Osada, T., et al. (2017). A new paradigm for drug-induced torsadogenic risk assessment using human iPS cell-derived cardiomyocytes. J. Pharmacol. Toxicol. Methods *84*, 111–127.
13. Blinova, K., Dang, Q., Millard, D., Smith, G., Pierson, J., Guo, L., Brock, M., Lu, H.R., Kraushaar, U., Zeng, H., et al. (2018). International multisite study of human-induced pluripotent stem cell-derived cardiomyocytes for drug proarrhythmic potential assessment. Cell Rep. *24*, 3582–3592.
14. Scott, C.W., Zhang, X., Abi-Gerges, N., Lamore, S.D., Abassi, Y.A., and Peters, M.F. (2014). An impedance-based cellular assay using human iPSC-derived cardiomyocytes to quantify modulators of cardiac contractility. Toxicol. Sci. *142*, 331–338.
15. Pointon, A., Harmer, A.R., Dale, I.L., Abi-Gerges, N., Bowes, J., Pollard, C., and Garside, H. (2015). Assessment of cardiomyocyte contraction in human-induced pluripotent stem cell-derived cardiomyocytes. Toxicol. Sci. *144*, 227–237.
16. Watanabe, H., Honda, Y., Deguchi, J., Yamada, T., and Bando, K. (2017). Usefulness of cardiotoxicity assessment using calcium transient in human induced pluripotent stem cell-derived cardiomyocytes. J. Toxicol. Sci. *42*, 519–527.
17. Saleem, U., van Meer, B.J., Katili, P.A., Mohd Yusof, N.A.N., Mannhardt, I., Garcia, A.K., Tertoolen, L., de Korte, T., Vlaming, M.L.H., McGlynn, K., et al. (2020). Blinded, Multicenter Evaluation of Drug-induced Changes in Contractility Using Human-induced Pluripotent Stem Cell-derived Cardiomyocytes. Toxicol. Sci. *176*, 103–123.
18. Yang, X., Pabon, L., and Murry, C.E. (2014). Engineering adolescence: maturation of human pluripotent stem cell-derived cardiomyocytes. Circ. Res. *114*, 511–523.
19. Ahmed, R.E., Anzai, T., Chanthra, N., and Uosaki, H. (2020). A Brief Review of Current Maturation Methods for Human Induced Pluripotent Stem Cells-Derived Cardiomyocytes. Front Cell Dev Biol *8*, 178.
20. Qu, Y., Feric, N., Pallotta, I., Singh, R., Sobbi, R., and Vargas, H.M. (2020). Inotropic assessment in engineered 3D cardiac tissues using human induced pluripotent stem cell-derived cardiomyocytes in the Biowire^{TM} II platform. J. Pharmacol. Toxicol. Methods *105*, 106886.
21. Takeda, M., Miyagawa, S., Fukushima, S., Saito, A., Ito, E., Harada, A., Matsuura, R., Iseoka, H., Sougawa, N., Mochizuki-Oda, N., et al. (2018). Development of in vitro drug-induced cardiotoxicity assay by using three-dimensional cardiac tissues derived from human induced pluripotent stem cells. Tissue Eng. Part C Methods *24*, 56–67.
22. Amano, Y., Nishiguchi, A., Matsusaki, M., Iseoka, H., Miyagawa, S., Sawa, Y., Seo, M., Yamaguchi, T., and Akashi, M. (2016). Development of vascularized iPSC derived 3D-cardiomyocyte tissues by filtration Layer-by-Layer technique and their application for pharmaceutical assays. Acta Biomater. *33*, 110–121.
23. Millard, D., Dang, Q., Shi, H., Zhang, X., Strock, C., Kraushaar, U., Zeng, H., Levesque, P., Lu, H.R., Guillon, J.M., et al. (2018). Cross-site reliability of human induced pluripotent stem cell-derived cardiomyocyte based safety assays using microelectrode arrays: results from a blinded CiPA pilot study. Toxicol. Sci. *164*, 550–562.
24. Rosati, B., Rocchetti, M., Zaza, A., and Wanke, E. (1998). Sulfonylureas blockade of neural and cardiac HERG channels. FEBS Lett. *440*, 125–130.

25. Hayakawa, T., Kunihiro, T., Dowaki, S., Uno, H., Matsui, E., Uchida, M., Kobayashi, S., Yasuda, A., Shimizu, T., and Okano, T. (2012). Noninvasive evaluation of contractile behavior of cardiomyocyte monolayers based on motion vector analysis. Tissue Eng. Part C Methods *18*, 21–32.

26. Khatib, S.Y., and Boyett, M.R. (2003). Effects of glyburide (glibenclamide) on myocardial function in Langendorff perfused rabbit heart and on myocardial contractility and slow calcium current in guinea-pig single myocytes. Mol. Cell. Biochem. *242*, 81–87.

27. Abe, Y., Ishisu, R., Onishi, K., Sekioka, K., Narimatsu, A., and Nakano, T. (1996). Calcium sensitization in perfused beating guinea pig heart by a positive inotropic agent MCI-154. J. Pharmacol. Exp. Ther. *276*, 433–439.

28. Ravenscroft, S.M., Pointon, A., Williams, A.W., Cross, M.J., and Sidaway, J.E. (2016). Cardiac non-myocyte cells show enhanced pharmacological function suggestive of contractile maturity in stem cell derived cardiomyocyte microtissues. Toxicol. Sci. *152*, 99–112.

29. Schocken, D., Stohlman, J., Vicente, J., Chan, D., Patel, D., Matta, M.K., Patel, V., Brock, M., Millard, D., Ross, J., et al. (2018). Comparative analysis of media effects on human induced pluripotent stem cell-derived cardiomyocytes in proarrhythmia risk assessment. J. Pharmacol. Toxicol. Methods *90*, 39–47.

30. Minami, I., Yamada, K., Otsuji, T.G., Yamamoto, T., Shen, Y., Otsuka, S., Kadota, S., Morone, N., Barve, M., Asai, Y., et al. (2012). A small molecule that promotes cardiac differentiation of human pluripotent stem cells under defined, cytokine- and xeno-free conditions. Cell Rep. *2*, 1448–1460.

31. Miki, K., Endo, K., Takahashi, S., Funakoshi, S., Takei, I., Katayama, S., Toyoda, T., Kotaka, M., Takaki, T., Umeda, M., et al. (2015). Efficient Detection and Purification of Cell Populations Using Synthetic MicroRNA Switches. Cell Stem Cell *16*, 699–711.

32. Li, J., Minami, I., Shiozaki, M., Yu, L., Yajima, S., Miyagawa, S., Shiba, Y., Morone, N., Fukushima, S., Yoshioka, M., et al. (2017). Human pluripotent stem cell-derived cardiac tissue-like constructs for repairing the infarcted myocardium. Stem Cell Reports *9*, 1546–1559.

33. Sasano, Y., Fukumoto, K., Tsukamoto, Y., Akagi, T., and Akashi, M. (2020). Construction of 3D cardiac tissue with synchronous powerful beating using human cardiomyocytes from human iPS cells prepared by a convenient differentiation method. J. Biosci. Bioeng. *129*, 749–755.